New Journal of Physics
The open access journal at the forefront of physics

Deutsche Physikalische Gesellschaft DPG IOP Institute of Physics

PAPER • OPEN ACCESS

A Fourier method for estimating potential energy and lateral forces from frequency-modulation lateral force microscopy data

To cite this article: T Seeholzer *et al* 2019 *New J. Phys.* **21** 083007

New Journal of Physics
The open access journal at the forefront of physics

Deutsche Physikalische Gesellschaft DPG
IOP Institute of Physics

Published in partnership with: Deutsche Physikalische Gesellschaft and the Institute of Physics

OPEN ACCESS

RECEIVED
24 May 2019

REVISED
27 June 2019

ACCEPTED FOR PUBLICATION
18 July 2019

PUBLISHED
5 August 2019

PAPER

A Fourier method for estimating potential energy and lateral forces from frequency-modulation lateral force microscopy data

T Seeholzer, O Gretz, F J Giessibl and A J Weymouth

Faculty of Physics, University of Regensburg, D-93053, Germany

E-mail: jay.weymouth@ur.de

Keywords: atomic force microscopy, lateral force microscopy, Pt(111), frequency-modulation lateral force microscopy (FM-LFM), force deconvolution

Supplementary material for this article is available online

Abstract

One mode of atomic force microscopy (AFM) is frequency-modulation AFM, in which the tip is driven to oscillate at its resonance frequency which changes as the tip interacts with the surface. Frequency-modulation lateral force microscopy (FM-LFM) is the variant of this technique in which the tip is oscillated along the surface. For an isolated adsorbate on a flat surface, the only signal in FM-LFM is caused by the short-range interaction with the adsorbate. Various deconvolution methods exist to convert the observed frequency shift into the more physically relevant parameters of force and energy. While these methods are often used for FM-AFM data, the high number of inflection points of FM-LFM data make standard deconvolution methods less reliable. In this article, we present a method based on Fourier decomposition of FM-LFM data and apply it to data taken of an isolated CO molecule on the Pt(111) surface. We probe the potential energy landscape past the potential energy minimum and show how over an adsorbate, the potential energy can be evaluated with a single FM-LFM image.

1. Introduction

One of the ongoing challenges in the field of atomic force microscopy (AFM) is to improve precision and spatial resolution. In this regard, frequency-modulation (FM) AFM has been quite successful [1, 2]. FM-AFM is a dynamic technique in which the tip is driven to oscillate at its resonance frequency. Interaction with the surface changes that resonance frequency and the resulting frequency shift, Δf, is one measure of the tip-sample interaction. This method has been used to push the boundaries of what was considered to be possible with force microscopy, having been used to image spin contrast at the atomic scale [3] and the internal structure of a molecular adsorbate [4].

Far from the surface, the cantilever acts as a spring with spring constant k and the tip oscillates at an unperturbed resonance frequency $f_0 = (1/2\pi)\sqrt{k/m^*}$, where m^* is the effective mass of the system. The frequency shift can be understood by considering the interaction between tip and sample as an additional spring with stiffness k_{ts}. When the tip oscillates in the x direction, $k_{ts} = -\mathrm{d}F_x/\mathrm{d}x = \mathrm{d}^2E/\mathrm{d}x^2$, where F_x is the component of force in the x direction, and E is the potential energy [1]. If it were the case that k_{ts} is constant over the tip oscillation, and with the approximation that $k \gg k_{ts}$, Δf can be written $\Delta f = (f_0/(2k))k_{ts}$. This is, however, rarely the case, especially when investigating physical phenomena that have length scales of tens of picometers. Instead, the exact formula must be considered [5, 6]:

$$\Delta f(x) = \frac{f_0}{2k}\langle k_{ts}(x)\rangle. \tag{1}$$

The effect of the tip's oscillation is taken account in the weighted force gradient $\langle k_{ts}\rangle(x)$:

$$\langle k_{ts}\rangle(x) = \frac{2}{\pi A^2}\int_{-A}^{A} k_{ts}(x+q)\sqrt{A^2-q^2}\,\mathrm{d}q. \tag{2}$$

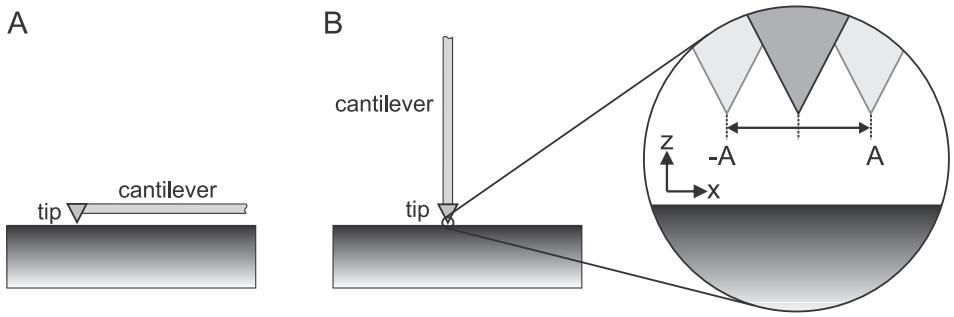

Figure 1. (A) The typical FM-AFM setup has a tip attached to a cantilever which is driven to oscillate normal to the surface. (B) The equivalent FM-LFM setup has a tip attached to a cantilever such that it oscillates laterally along the surface. The magnitude of oscillation is A. Our cantilever has a length of 1.23 mm, and the tip is driven to oscillate with amplitudes around $A \approx 100$ pm.

In this equation, q is a variable of integration describing the oscillation of the tip around a center position x with an amplitude A. The challenge, therefore, is to work backwards from the observed Δf to determine the integrand and with it force and energy.

The two most common deconvolution methods used to convert the Δf data of FM-AFM experiments to force and energy are the Sader–Jarvis method [7] and the Matrix method [6]. Both of these methods take a line of data along the direction of the tip oscillation from a point where the forces and energy can be assumed to be zero (i.e. far from the sample) to the distance of interest. The Matrix method is a method that starts by describing the transformation from force to Δf as a matrix which can be inverted. In the Sader–Jarvis method, the force curve is modeled as a sum of exponential functions (Laplace transform). It then applies an approximation to invert the Δf signal to reconstruct force and potential energy. Recently, a problem has been identified with both of these methods in that they can suffer from being ill-posed for a given force curve and amplitude [8, 9]. The mathematical problem of reconstructing force and energy for an observed Δf dataset can have multiple solutions, some of which are non-physical.

In FM lateral force microscopy (LFM) the tip oscillates parallel to the surface [10, 11]. We accomplish this by rotating our sensor, as sketched in figure 1. This dynamic mode is the natural extension to the successful contact-mode LFM [12, 13]. In this configuration, the measurement is not sensitive to long-range van der Waals and electrostatic forces that are normal to the surface, but rather to interactions with a strong lateral component [14, 15] for example, from a nearby step edge [16]. This makes frequency-modulation lateral force microscopy (FM-LFM) ideal for investigating the short-range interactions between the tip and an isolated adsorbate on a flat terrace [17]. One challenge with FM-LFM data is the deconvolution from Δf back to the more physical descriptions of a system of force and energy. The mathematical description of the relation between force, energy and frequency shift remains the same as it is for FM-AFM and in principle has the same challenges associated with it. This is true in our setup, where we use a qPlus sensor [18] in the first flexural mode [11]. When lateral forces are detected with the torsional mode of a soft sensor [10, 19, 20], then the motion of the normal mode must also be taken into account [14]. Even when only the first flexural mode is laterally excited, the typical Δf curve for FM-LFM data along the direction of tip oscillation (required to calculate force and energy) has many more inflection points than typical FM-AFM data, causing it to fall directly into the set of curves for which the force and energy deconvolution by either the Sader–Jarvis method or Matrix method is ill-posed (see figure 1(b) in [9]).

Another method to estimate the potential energy landscape that corresponds to Δf data is to start from a model potential with a given set of parameters (e.g. a Gaussian function where the width and depth are free parameters). If the model is appropriate, then the problem of ill-posedness is avoided as Δf can be calculated directly from the model, and the parameters can be chosen to minimize the least-squares error between the experimental signal and the model output. The problem with models based, e.g. on Morse interactions [17] or on a sum of Gaussian functions [21] is that they are not generally applicable. This has prompted us to implement a force and energy deconvolution method that is applicable for potential energy curves that are periodic. While this is rarely the case for FM-AFM data, it is often the case for FM-LFM data. In particular, when scanning laterally above an adsorbate on a flat terrace, as sketched in figure 2(A), the potential energy far from the adsorbate on either side is the same. This is also true for periodic systems including surface reconstructions.

In this article, we introduce a method of force and energy deconvolution that is based upon a Fourier decomposition, building on an idea that we introduced in [22]. In short, if the frequency shift is periodic, then it can be decomposed into a Fourier series. The coefficients describing Δf directly relate to the coefficients that describe the periodic potential energy, and therefore can directly yield the potential energy and lateral force. The derivation is shown in section 2. We then apply our Fourier method in section 3 to evaluate the lateral forces above a single CO molecule on Pt(111).

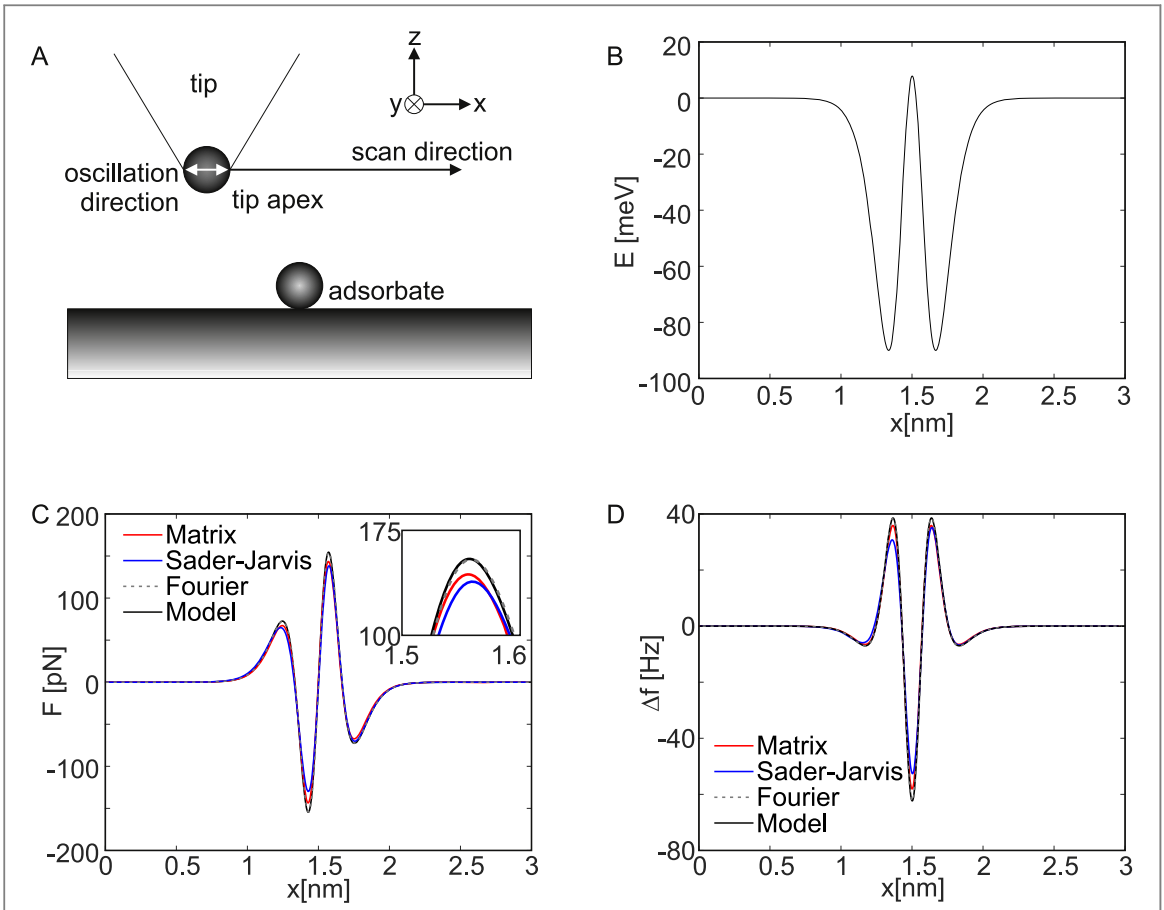

Figure 2. (A) Schematic of the FM-LFM sensor. Tip oscillation direction is shown with a white double-headed arrow. The scan direction is taken in the same direction, a requirement to convert the observed Δf into force and energy. The interaction between tip and surface was considered by a Morse interaction between the apex tip atom and a surface particle. x, y and z are here defined for the remainder of the article. (B) The calculated potential energy curve as a function of the lateral position. (C) The calculated frequency shift was converted back into force and the output of various deconvolution methods compared to the force from the model. (D) From the deconvoluted forces, the frequency shift was calculated and compared to the model.

1.1. The challenge with FM-LFM data

As noted above, one of the hallmarks of FM-LFM data are the many inflection points along a Δf curve which can cause the standard deconvolution methods to be unreliable [8]. We can model the interaction between a tip apex and an adsorbate with a Morse potential to illustrate these challenges. The inaccuracy of deconvolution methods has been previously discussed and estimated in the context of FM-AFM data [7, 23, 24]; here we consider inaccuracy in the context of FM-LFM data. Figure 2(B) shows the calculated potential energy curve for a tip moving above an adsorbate with parameters $\sigma = 300$ pm and $\lambda = 70$ pm, at a relative height above the center of the adsorbate of 250 pm.

From the potential energy curve, the frequency shift can be calculated via equations (2) and (1). This calculation requires the spring constant of the sensor, here given to be $k = 1150$ N m^{-1}, the amplitude of the tip oscillation, here chosen to be $A = 20$ pm, and the center frequency, here chosen to be $f_0 = 42\,000$ Hz. It is shown as a black line in figure 2(D). The calculated Δf line is 3 nm long and consists of 1024 data points. These values have been chosen as they are typical values for such an experimental setup.

From the model, we can directly calculate the lateral force component as the tip passes over the adsorbate, shown in figure 2(C) as a black line. From the ideal Δf curve, we applied the Sader–Jarvis method, the Matrix method, and our Fourier method to calculate the lateral forces. The results are shown in figure 2(C), where the Fourier method reproduces the force, and both other methods are inaccurate around the maxima (shown in the inset) and minima: The actual value of force at the maximum is 154.5 pN. The Sader–Jarvis method has an error of 16.3 pN; the Matrix method has an error of 11.0 pN and the Fourier method has an error of 0.3 pN. Both the Sader–Jarvis method and the Matrix method are designed to deconvolute FM-AFM data from a point far from the surface to a point close to the surface. We integrated from a large value of x to a smaller value. At the global minimum, the inaccuracy of the Sader–Jarvis method is 24.7 pN. The inaccuracy of the Matrix method can be decreased by increasing the density of data points [24].

In [9], two criteria are proposed to judge whether a force curve is ill-posed for a given amplitude range at each of its inflection points. The force curve from the Morse model, shown in figure 2(C), has five inflection

points. For this curve, the inflection points at 1.8 and 1.2 nm are ill-posed for amplitudes between 70 and 913 pm; the inflection points at 1.6 and 1.4 nm are ill-posed for amplitudes between 48 and 681 pm; and the inflection point at 1.5 nm is ill-posed for amplitudes between 42 and 748 pm. Already this points to a large challenge for converting FM-LFM data into force and energy if a typical force curve is ill-posed for such a large range of typically-used amplitudes. Nonetheless, we chose to generate the Δf with an amplitude outside of this ill-posed range for a fair comparison.

Even with our amplitude of $A = 20$ pm, and a density of 1024 data points/3 nm, the force estimates of the Sader–Jarvis and the Matrix method had a significantly higher error than the Fourier method when compared to the model force curve, as shown in figure 2(C). When converting these force curves back to a Δf signal, only the Fourier method reproduced the model Δf curve. This test data already indicate a strong advantage of the Fourier method for deconvolving FM-LFM data.

2. Fourier-deconvolution based method to estimate force and energy

This section will again use the coordinate convention defined in figure 2(A), where z is the vertical component, x is the direction of the tip oscillation, and y is perpendicular to both z and x. Deconvolution to force and energy requires a line of FM-LFM data along the direction of tip oscillation, or $\Delta f(x)$, for a given y, z position. We consider a line of length L that is long enough so that the effect of the adsorbate on the measurement is negligable at the ends ($x = 0$ m and $x = L$), and therefore the potential energy at either end of the line must be the same. As the z and y values are constant for this line, we write $E_{y,z}(x) := E(x, y, z)$. $E_{y,z}(x)$ can be written as a Fourier series with components a_n and b_n:

$$E_{y,z}(x) = \sum_{n=1}^{N} a_n \sin\left(n\frac{2\pi}{L}x\right) + b_n \cos\left(n\frac{2\pi}{L}x\right). \tag{3}$$

The coefficients a_n and b_n are functions of y and z, and could also be written $a_n = a_n(y, z)$ and $b_n = b_n(y, z)$. The sum is taken to N, whose maximal value is given by the Nyquist frequency. Although in this case wavenumber is a more appropriate term than frequency, the Nyquist frequency is a general term given to half of the sampling rate. In this case, the highest sampled wavenumber is half of the number of data points divided by the length of the line L. Furthermore, the $n = 0$ term can be neglected as the zero position of potential energy is set at a given point, for example, far from the adsorbate.

The lateral force (i.e. force component in the x-direction) follows as $F_{y,z}(x) = -\mathrm{d}E_{y,z}(x)/\mathrm{d}x$:

$$F_{y,z}(x) = \sum_{n=1}^{N} -a_n\left(\frac{2\pi n}{L}\right)\cos\left(n\frac{2\pi}{L}x\right) + b_n\left(\frac{2\pi n}{L}\right)\sin\left(n\frac{2\pi}{L}x\right). \tag{4}$$

And the force gradient $k_{\mathrm{ts},y,z}(x) = -\mathrm{d}F_{y,z}(x)/\mathrm{d}x$:

$$k_{\mathrm{ts},y,z}(x) = \sum_{n=1}^{N} -a_n\left(\frac{2\pi n}{L}\right)^2\sin\left(n\frac{2\pi}{L}x\right) - b_n\left(\frac{2\pi n}{L}\right)^2\cos\left(n\frac{2\pi}{L}x\right). \tag{5}$$

Inserting equation (5) into equation (2) to take into account the tip oscillation and derive the weighted force gradient yields

$$\langle k_{\mathrm{ts}}\rangle_{y,z}(x) = \sum_{n=1}^{N} -a_n\left(\frac{4\pi n}{AL}\right)\sin\left(\frac{2\pi n}{L}x\right)J_1\left(\frac{2\pi nA}{L}\right) - b_n\left(\frac{4\pi n}{AL}\right)\cos\left(\frac{2\pi n}{L}x\right)J_1\left(\frac{2\pi nA}{L}\right) \tag{6}$$

J_1 is the Bessel function of the first kind and first order.

Assuming that the data start and end with an average of 0 Hz, a line of FM-LFM data at a given z height and constant y position, $\Delta f_{y,z}(x) := \Delta f(x, y, z)$, can be decomposed as a Fourier series with components α_n and β_n:

$$\Delta f_{y,z}(x) = \sum_{n=1}^{N} \alpha_n \sin\left(n\frac{2\pi}{L}x\right) + \beta_n \cos\left(n\frac{2\pi}{L}x\right). \tag{7}$$

Comparing equation (6) with equation (7) via equation (1), α_n and β_n directly yield a_n and b_n:

$$a_n = -\alpha_n \frac{2k}{f_0}\left(\frac{AL}{4\pi n}\right)\frac{1}{J_1\left(\frac{2\pi nA}{L}\right)}, \tag{8}$$

$$b_n = -\beta_n \frac{2k}{f_0}\left(\frac{AL}{4\pi n}\right)\frac{1}{J_1\left(\frac{2\pi nA}{L}\right)} \tag{9}$$

a_n and b_n can be used to write an analytic expression for lateral force via equation (4) and potential energy via equation (3).

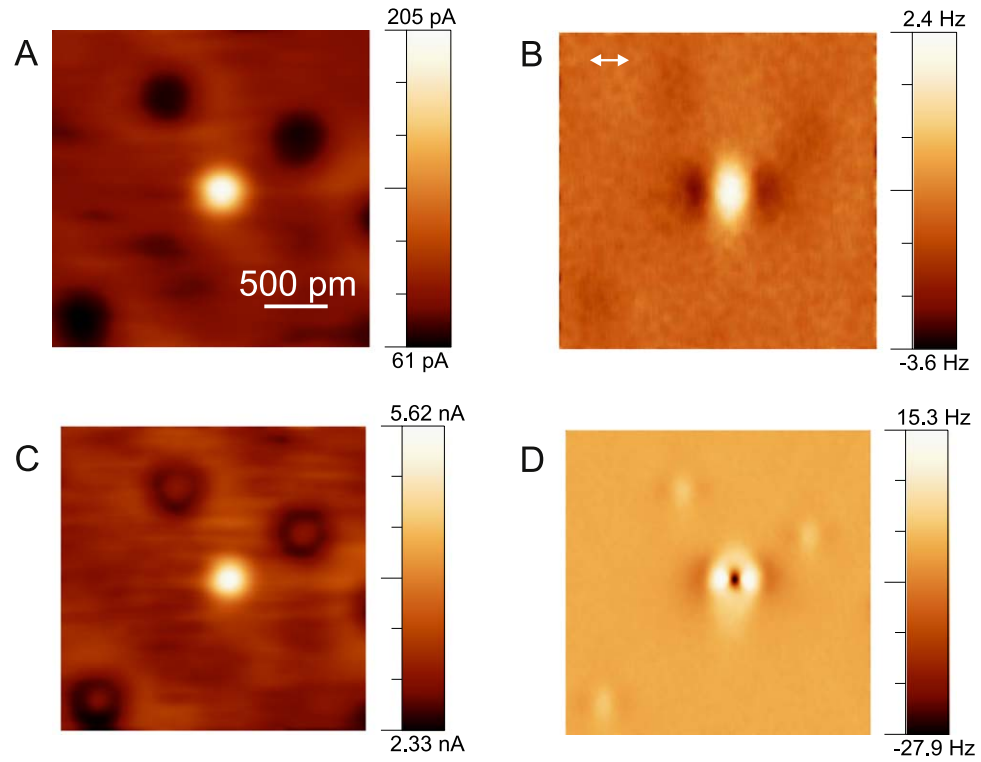

Figure 3. STM and FM-LFM images of a CO molecule and three carbon defects on Pt(111). 2 meV bias voltage. (A) and (B), 150 pm above closest approach. (C) and (D), closest approach. The direction of tip oscillation is marked by a white double-headed arrow in (B).

2.1. Numeric implementation

To implement the above equations, we used a scalar projection of the data onto the relevant sine or cosine functions. That is, α_n was estimated by a numeric integral of $\Delta f\,(x) \cdot \sin\,(2\pi nx/L)$ divided by the appropriate normalization factor, in this case $L/2$. An implementation of this function in MATLAB is provided as a download from the supplemental material available online at stacks.iop.org/NJP/21/083007/mmedia.

Although the formulae presented in the above section are mathematically correct, numeric implementation of them is another challenge. When converting from α_n and β_n to a_n and b_n, a division by $J_1\left(\frac{2\pi nA}{L}\right)$ is required. The first zero-crossing of J_1 function is at

$$\frac{2\pi nA}{L} \approx 3.8317. \tag{10}$$

The number of components before this first zero-crossing is

$$n < 3.8317\frac{L}{2\pi A} \approx \frac{L}{2A}. \tag{11}$$

For a line scan of 2 nm acquired with an oscillation amplitude of 50 pm, this results in 20 components. As L increases, so does the number of components before the first crossing. We have seen that increasing L leads to less ringing in the potential energy calculations.

In general, a band-pass filter can be used to remove the unwanted higher-order components. Although this is not necessary when calculating potential energy, we have found the higher order components to play a large role in the force estimate.

3. Lateral forces over a CO molecule on a Pt(111) surface

We applied the Fourier method to determine the potential energy between the tip and isolated CO molecules on the Pt(111) surface over a range of tip-sample distances. The Pt(111) sample was cleaned with repeated sputter and anneal cycles until the defect density was considered to be low enough. Residual carbon defects were observed in the STM images as atomic-scale defects of lower conductance [25], whereas CO molecules were observed as atomic-scale features with higher conductance [26, 27]. Data were collected in a low-temperature (He bath) CreaTec GmbH STM/AFM system with home-built FM-LFM sensors. For the data presented here,

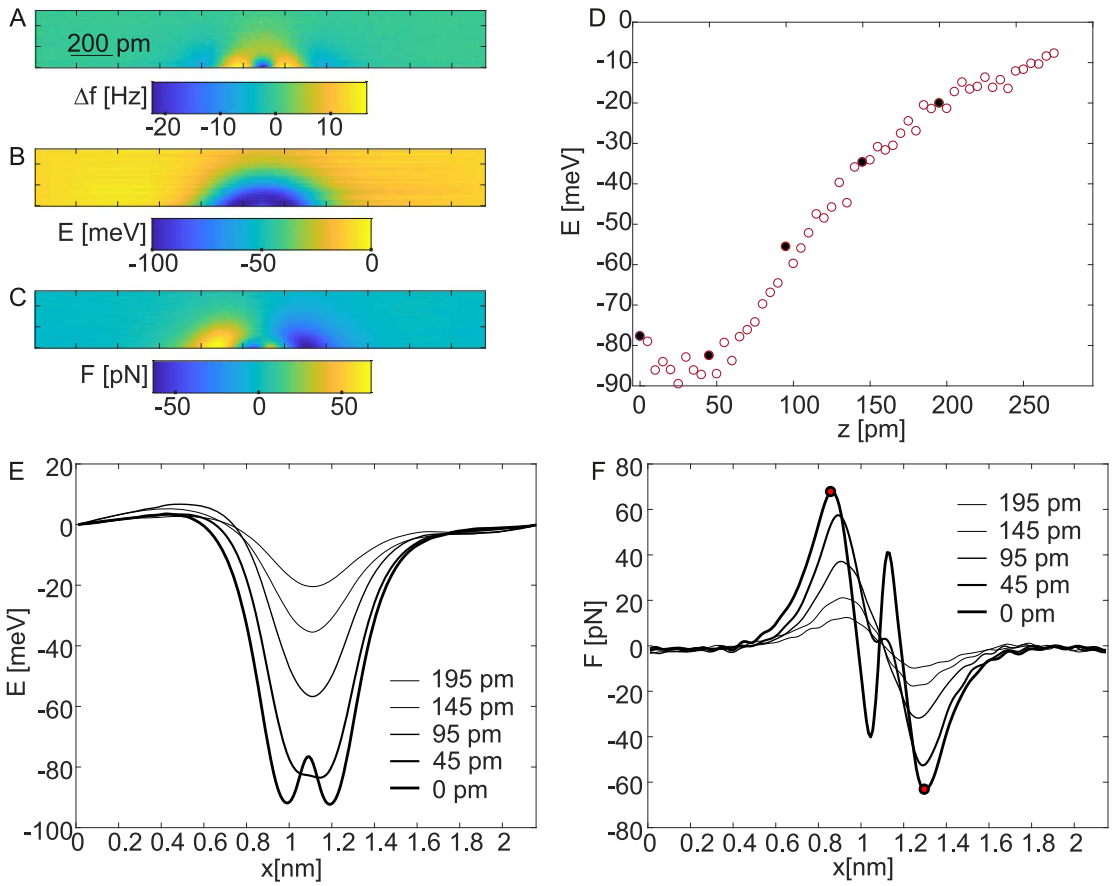

Figure 4. (A) Δf data as a function of height over the CO molecule shown in figure 3. The data were converted with the Fourier method to (B) energy and (C) lateral force. (D) Energy as a function of tip-sample distance above the adsorbate showing a potenital energy minimum of approximately 87 meV. (E) Line scans of the potential energy at various height. Height is relative to the closest approach in this dataset. (F) Corresponding force profiles. At the closest approach in this dataset, the maximum and minimum forces (marked by red dots) were 68 pN and −63 pN.

the amplitude of oscillation was 42.5 pm. The scan direction was adjusted so that the oscillation direction is in the fast scan direction. For data shown in figures 3, 4(A) and 5(A), this corresponds to the horizontal direction.

Constant-height STM and corresponding FM-LFM images are shown in figure 3. The CO molecule appears as a bright feature in the STM image. The tip oscillation is shown by the double-headed arrow in figure 3(B). The amplitude of the oscillation was much smaller than indicated by the double-headed arrow, and therefore has little effect on the STM image. In the simultaneously-acquired FM-LFM image the CO appears as a dark-bright-dark feature along the direction of the tip oscillation. This signature is indicative of attractive interaction between the tip and sample [21].

Closer to the surface the carbon defects start to show a brighter feature, shown in figure 3(C). In the FM-LFM image, shown in figure 3(D), the magnitude of the Δf is much higher and a new feature can be seen in the center. This additional sharp decrease in Δf in the center is a signature of a repulsive feature [21].

We collected a three-dimensional set of data above the CO molecule. Figure 4(A) shows the Δf data as a function of both lateral position in the direction of the tip oscillation and vertical position. For each line, we applied the Fourier method to determine the potential energy, shown in figure 4(B). At each height, we set the potential energy to zero far from the adsorbate. This convention is common in FM-AFM studies of isolated adsorbates and is typically performed with the on–off technique [28]. The resulting lateral force component (force component in the direction of the tip oscillation) is shown in figure 4(C). Line scans at various tip-sample heights of potential energy and lateral force are given in figures 4(E) and (F).

The potential energy directly over the center of the CO molecule can be plotted as a function of vertical height, shown in figure 4(D), where a minimum of approximately 87 meV can be seen. To put this value into context, we can compare to previous studies of a tip interacting with a single CO adsorbate. On a Cu(111) substrate, a CO-terminated tip yielded a potential energy minimum of approximatey 10 meV, and the energy minimum between a metal tip and a CO molecule could not be reached [29]. The energy minimum between a metal tip and a CO molecule on the Cu(111) surface has been estimated to be 200 meV [30].

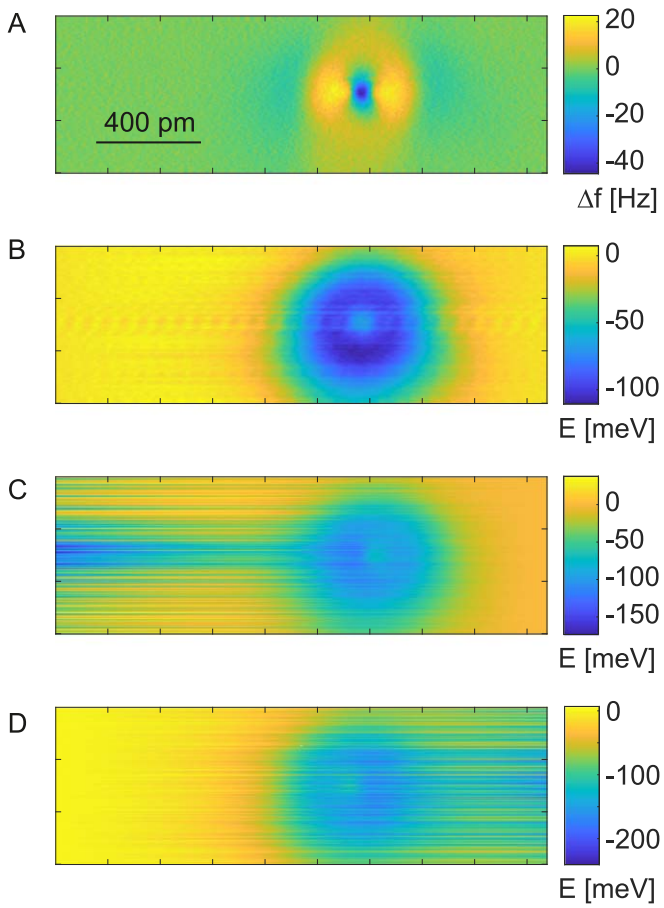

Figure 5. (A) FM-LFM image of a single CO molecule. (B) Corresponding potential energy image calculated by the Fourier method. (C) Potential energy image calculated with the Sader–Jarvis method starting the integration from the right-hand side. (D) Potential energy calculated with the Sader–Jarvis method starting from the left-hand side.

Finally, one of the great appeals of FM-LFM is that with one single image, the corresponding potential energy image can be directly calculated. For a potential energy image to be evaluated with FM-AFM, Δf data must be collected—for each x, y position—over a range from the height at which the potential energy image is desired to a point where the short-range contribution is no longer present. Acquiring a three-dimensional dataset usually takes hours, in comparison to the minutes it takes for a single image. A FM-LFM image is shown in figure 5(A), with a very sharp feature in the center of the CO molecule with a FWHM (full width at half maximum) of 63 pm. The data can then be converted, line-by-line, into potential energy, shown in figure 5(B). Here the shape of the molecule with the attractive ring and the potential energy bump in the middle, most likely caused by Pauli repulsion, can be seen.

Figure 5(C) shows the potential energy calculated from the Sader–Jarvis method. The integration direction was from right to left. Past the many inflection points over the center of the CO, the energy estimate becomes less reliable. This is a hard example of the inaccuacies discussed in figure 2(C), where the inaccuracies get larger over further inflection points. Similar problems can be seen when integrating from left to right, as shown in figure 2(D). It is also an excellent example that illustrates the advantages of the Fourier method.

4. Conclusions

With the continuous development of force microscopy, new techniques are required that can convert the measured signal into the physically meaningful quantities of force and energy. The Sader–Jarvis method is based around a Laplace transform, which represents a function as a series of decreasing exponential functions [7]. This is a logical starting point when considering $\Delta f(z)$ curves in FM-AFM data, but not the ideal choice of basis functions when considering FM-LFM data. We have implemented a method for FM-LFM data based on Fourier decomposition that enforces periodic boundary conditions in the potential energy. This takes into account the physical setup encountered in LFM experiments in which data is acquired of an isolated adsorbate on a flat terrace. The spatial resolution in the FM-LFM data that we show is on the order of tens of picometers. With the

Fourier method, we demonstrated the unique power of FM-LFM: to evaluate the potential energy landscape from a single image.

Acknowledgments

We would like to thank K Pürckhauer and A Merkel for their help constructing the FM-LFM sensors, F Huber for providing software to test the force deconvolution for ill-posed behaviour and commenting on the manuscript, and E Riegel and A Peronio for their help preparing the Pt(111) surface. AJW and OG would like to thank the Deutsche Forschungsgemeinschaft (grant number WE5053/2-1, 'Locally mapping conductance and potential energy of a donor-acceptor system') for funding.

ORCID iDs

T Seeholzer https://orcid.org/0000-0001-7026-7868
O Gretz https://orcid.org/0000-0002-1046-172X
F J Giessibl https://orcid.org/0000-0002-5585-1326
A J Weymouth https://orcid.org/0000-0001-8793-9368

References

[1] Albrecht T R, Grütter P, Horne D and Rugar D 1991 *J. Appl. Phys.* **69** 668
[2] Giessibl F J 1995 *Science* **267** 68–71
[3] Kaiser U, Schwarz A and Wiesendanger R 2007 *Nature* **446** 522–5
[4] Gross L, Mohn F, Moll N, Liljeroth P and Meyer G 2009 *Science* **325** 1110–4
[5] Giessibl F J 1997 *Phys. Rev.* B **56** 16010
[6] Giessibl F J 2001 *App. Phys. Lett.* **78** 123
[7] Sader J E and Jarvis S P 2004 *Appl. Phys. Lett.* **84** 1801–3
[8] Sader J E, Hughes B D, Huber F and Giessibl F J 2017 arXiv:1709.07571
[9] Sader J E, Hughes B D, Huber F and Giessibl F J 2018 *Nat. Nanotechnol.* **13** 1088–91
[10] Pfeiffer O, Bennewitz R, Baratoff A, Meyer E and Grütter P 2002 *Phys. Rev.* B **65** 161403
[11] Giessibl F J, Herz M and Mannhart J 2002 *Proc. Natl Acad. Sci. USA* **99** 12006–10
[12] Meyer G and Amer N M 1990 *Appl. Phys. Lett.* **57** 2089
[13] Mate C, McClelland G, Erlandsson R and Chiang S 1987 *Phys. Rev. Lett.* **59** 1942–5
[14] Kawai S, Glatzel T, Koch S, Such B, Baratoff A and Meyer E 2010 *Phys. Rev.* B **81** 085420
[15] Weymouth A J 2017 *J. Phys.: Condens. Matter* **29** 323001
[16] Kawai S, Canova F F, Glatzel T, Hynninen T, Meyer E and Foster A S 2012 *Phys. Rev. Lett.* **109** 146101
[17] Weymouth A J, Hofmann T and Giessibl F J 2014 *Science* **343** 1120
[18] Giessibl F J 1998 *Appl. Phys. Lett.* **73** 3956
[19] Federici Canova F, Kawai S, De Capitani C, Kan'No K I, Glatzel T, Such B, Foster A S and Meyer E 2013 *Phys. Rev. Lett.* **110** 203203
[20] Naitoh Y, Turanský R, Brndiar J, Li Y J, Štich I and Sugawara Y 2017 *Nat. Phys.* **13** 663
[21] Weymouth A, Riegel E, Matencio S and Giessibl F 2018 *Appl. Phys. Lett.* **112** 181601
[22] Weymouth A J, Meuer D, Mutombo P, Wutscher T, Ondracek M, Jelinek P and Giessibl F J 2013 *Phys. Rev. Lett.* **111** 126103
[23] Dagdeviren O E, Zhou C, Altman E I and Schwarz U D 2018 *Phys. Rev. Appl.* **9** 44040
[24] Welker J, Illek E and Giessibl F J 2012 *Beil. J. Nanotechnol.* **3** 238–48
[25] Wiebe J, Meier F, Hashimoto K, Bihlmayer G, Blügel S, Ferriani P, Heinze S and Wiesendanger R 2005 *Phys. Rev.* B **72** 2–5
[26] Stroscio J A and Eigler D M 1991 *Science* **254** 1319–26
[27] Yang H J, Minato T, Kawai M and Kim Y 2013 *J. Phys. Chem.* C **117** 16429–37
[28] Ternes M, González C, Lutz C, Hapala P, Giessibl F J, Jelínek P and Heinrich A 2011 *Phys. Rev. Lett.* **106** 016802
[29] Sun Z, Boneschanscher M P, Swart I, Vanmaekelbergh D and Liljeroth P 2011 *Phys. Rev. Lett.* **106** 046104
[30] Welker J and Giessibl F J 2012 *Science* **336** 444–9